

COMPARISON OF CIRCULAR AND RECTANGULAR COIL TRANSFORMER PARAMETERS FOR WIRELESS POWER TRANSFER BASED ON FINITE ELEMENT ANALYSIS

¹Daniel Ongayo and ²Moin Hanif, *Member, IEEE*

Department of Electrical Engineering, University of Cape Town, Cape Town, South Africa
e-mail: ¹ongdan001@myuct.ac.za, ²moin.hanif@uct.ac.za

Abstract – The major parameters of transformers used in wireless Power Transfer (WPT) are self inductance, mutual inductance and coefficient of coupling. Due to unique and complex nature of these transformers, determining these parameters by calculation has limitations which however can be overcome by use of Finite Element Analysis (FEA). This paper presents and compares the parameters of a circular and rectangular coil transformer modelled under different conditions using Ansys Maxwell software. An introduction to WPT system and its transformer model is also presented.

Keywords – Ansys Maxwell, Coefficient of coupling, Finite element analysis, Mutual inductance, Wireless power transfer, Self inductance.

I. INTRODUCTION

WPT system has recently attracted a lot of research interest mainly due to its application in charging electric vehicles, mobile phones and biomedical implants.

Inductive power transfer (IPT) is one of the WPT technique use to transfer power through mutual coupling between coils in a manner similar to that in conventional transformers, however power is magnetically transferred from source to the load over large air gaps. The efficiency of power transfer in this system highly depends on the construction of the transformer used [1]-[4].

The key parameters of these transformers which are of significant importance in the analysis of the WPT system are self- and mutual-inductance which make up the coils to establish parameters such as the coupling coefficient.

Calculations of these parameters is limited to simple air-core transformers [5]. With ferrite core and other materials incorporated in the tranformer design to improve the power transfer efficiency, calculations of the parameters becomes more complicated. These limitations may be overcome by use of finite element analysis.

Using FEA software Ansys Maxwell, this paper compares the parameters of circular and rectangular coil transformers under three different conditions: coreless transformer, ferrite–core transformer unshielded and ferrite–core transformer with Aluminium shield.

Section I of this paper presents an introduction to IPT transformer model with key expressions relating the IPT transformer parameters. FEA modeling and simulation results for circular and rectangular coil transformers are presented in Section III and IV respectively.

II. IPT TRANSFORMER MODEL

An IPT transformer can be modelled from the theory of mutual inductance as shown in Fig. 1. Here, R_1 is primary winding resistance, R_2 , secondary winding resistance, L_1 , primary winding self-inductance, L_2 , secondary winding self inductance and M mutual inductance. A relation between M and coefficient of coupling k can be expressed as [2]:

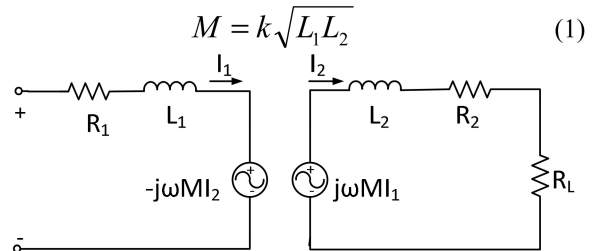


Fig. 1. IPT transformer coupling model.

Assuming sinusoidal voltages and currents, the voltage induced in the secondary side due to the current of the primary side is equal to $j\omega MI_1$. In the same way, the voltage reflected in the primary side due to the current of the secondary side is equal to $-j\omega MI_2$, where ω is the operational frequency. R_L represents a resistive load [6]-[9].

With reference to leakage inductances, the IPT transformer equivalent circuit may be represented as in Fig. 2.

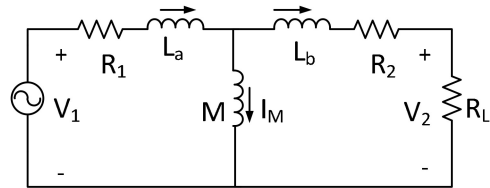


Fig. 2. Equivalent circuit of an IPT transformer.

This form of representation is more suitable for the transformer's characteristics and performance analysis. I_M is the magnetizing current, L_a , L_b and M are the primary leakage inductance, secondary leakage inductance and mutual inductance respectively. The relationship between L_a , L_b and M is given by:

$$L_a = L_1 - M \quad (2)$$

$$L_b = L_2 - M \quad (3)$$

The performance of an IPT secondary coil (L_2), commonly referred to as the pickup coil is primarily determined from two parameters; the open circuit voltage (V_{oc}) induced in the

pickup coil at frequency (ω) due to the primary current (I_1) and its short circuit current (I_{sc}) is given by [10]:

$$V_{oc} = j\omega MI_1 \quad (4)$$

$$I_{sc} = MI_1 / L_2 \quad (5)$$

I_{sc} is the maximum current from V_{oc} limited by ωL_2 , the impedance of the pickup coil inductance.

The product of these two parameters results in the uncompensated VA of the pickup (P_{su}) given by [11], [12], [13]:

$$P_{su} = V_{oc} I_{sc} = \omega I_1^2 \frac{M^2}{L_2} \quad (6)$$

Without compensation, the maximum power that can be drawn from a pickup is $P_{su}/2$, which is generally not sufficient.

In order to improve the available power, the pickup inductor is compensated with capacitors such that it resonates at or near the frequency of the primary coil. Normally, the compensation capacitor (C_2) is applied either directly in series or parallel, although parallel tuned pickups are more common due to their current limiting capabilities. The ac tuning causes resonant current to flow in the tuned circuit comprising L_2 and C_2 . The resulting secondary current is boosted by the secondary coil quality factor (Q) for series compensation while for parallel compensation, the secondary voltage is boosted.

$$Q = \frac{\omega L_2}{R_2} \quad (7)$$

When compensated the power output (P_{out}) of an IPT can be expressed as [14]:

$$P_{out} = P_{su} Q = V_{oc} I_{sc} Q = \omega I_1^2 \frac{M^2}{L_2} Q \quad (8)$$

This can also be written in terms of the VA at the input of the transmitter pad as [15]:

$$P_{out} = V_{in} I_1 k^2 Q \quad (9)$$

Where V_{in} is the primary coil terminal voltage and I_1 its input current.

As shown in (8), the output power depends on the power supply (ωI_1^2), magnetic coupling (M^2/L_2) and pick up quality factor (Q). The operational frequency and current of the power supply are limited by those switching devices presently available, and both have to be balanced against switching and copper losses.

III. CIRCULAR COIL TRANSFORMER MODELLING AND ANALYSIS

In this section, 3-D FEA software Ansys Maxwell is used to model circular coil transformers under three different configurations in order to determine the model which results in optimal parameters suitable for wireless power transfer.

A. FEA Modelling

A circular coil transformer with the dimensions in Table I was modelled using Ansys Maxwell.

TABLE I
Circular coil Transformer dimensions

Winding no. of turns	22
Winding Diameter	Outer-170 mm, Inner-60 mm
Conductor Thickness	2 mm
Ferrite Bars	6 bars: 65x20x5mm
Aluminum Shield	Diameter-190 mm, thickness-2 mm

Three models of the inductive power transformer designed in Ansys Maxwell are shown in Fig. 3 to Fig. 5.

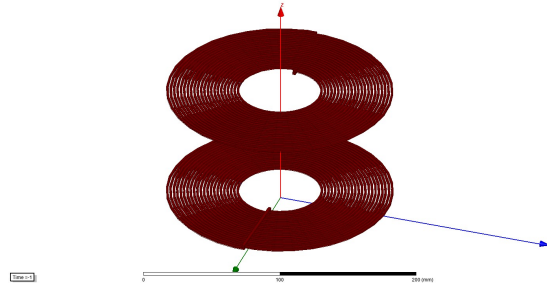


Fig. 3. Circular Coreless transformer model

Coreless transformer model (Fig. 3) consists of primary and secondary coil with copper windings only. Coreless transformers are generally not suitable for high power applications where ferrous materials are in close proximity to the system due to eddy and hysteresis losses.

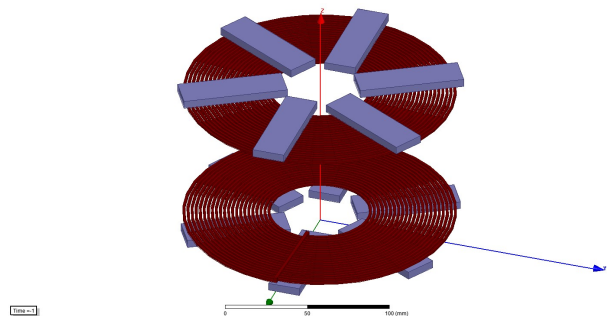


Fig. 4. Circular transformer model with Ferrite core only

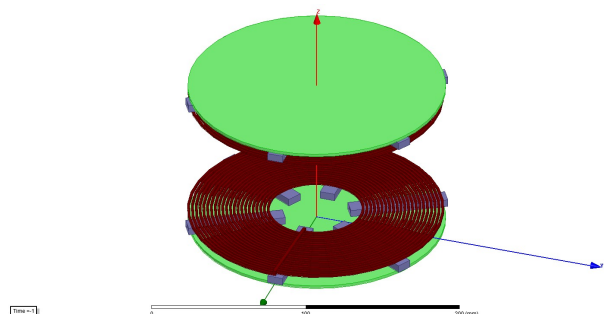


Fig. 5. IPT transformer model with Ferrite core and Aluminum shield

Field shaping with ferrite (Fig. 4) constrains flux to desired paths improving coupling and consequently preventing excessive energy loss in surrounding materials due to leakage

magnetic field, which also needs to be considered for safety reasons. Conventional techniques use pot cores, U-shaped cores, ferrite discs or plates whose designs are comparatively fragile and expensive due to geometry of the large pieces of ferrite required to achieve the desired flux path [16]. Aluminium shield placed above the receiving coil and below the transmitting coil (Fig. 5) is used to reduce the leakage of the magnetic field by limiting its distribution to a specified region. In so doing the risk of human exposure to harmful radiation is reduced.

B. Simulation results from Ansys Maxwell

In order to determine the transformer key parameters, the models of Fig. 3 to Fig. 5 were simulated in Ansys Maxwell from a 240 volts, 20 kHz a.c sinusoidal voltage. The results from simulation are shown in Table II, III and IV where d is the distance between the transmitting and receiving coil, L_1 Primary coil self-inductance, L_2 secondary coil self-inductance, M mutual inductance and k coefficient of coupling.

TABLE II
Simulation results from Circular Coreless Transformer

d, mm	$L_1, \mu\text{H}$	$L_2, \mu\text{H}$	$M, \mu\text{H}$	k
100	57.82	58.03	5.63	0.097
70	56.13	56.27	8.22	0.15
50	50.08	49.95	13.91	0.28

TABLE III
Simulation results from Circular Ferrite-core Transformer with no shield

d, mm	$L_1, \mu\text{H}$	$L_2, \mu\text{H}$	$M, \mu\text{H}$	k
100	92.96	93.48	12.04	0.129
70	92.61	92.39	19.20	0.21
50	94.53	93.94	41.45	0.44

TABLE IV
Simulation results from Circular Ferrite-core Transformer with Aluminum shield

d, mm	$L_1, \mu\text{H}$	$L_2, \mu\text{H}$	$M, \mu\text{H}$	k
100	89.60	90.75	10.90	0.121
70	89.29	88.65	17.43	0.20
50	94.35	92.47	40.04	0.43

From the results, it is notable that when d changes, L_1 and L_2 variation is small as compared to that of M . In all the three scenarios M and k increase as the distance between the two coils is reduced. A larger M and k in (8) and (9) means more power is transferred to the output. The presence of ferrite core results in larger values of M and k as compared to coreless transformer. Although coreless transformer would be light and cheap, its low mutual inductance and coefficient of coupling limits its application for high and efficient power transfer. Comparison between the shielded and unshielded

transformers reveals that there is marginal change in the parameters especially M and k . The reduction of M and k due to shielding is negligible.

The magnetic field density plot for the three transformers at 50 mm separation between the transmitting and receiving coil is shown fig. 6 to fig. 8

The magnetic field density plot scale on the left of each diagram indicates the range of the strength of the magnetic field density with the bottom blue representing the lowest value and the top red the highest value.

The strongest field density is observed in Fig. 7 and the lowest in Fig. 6. This is due to the presence of the ferrite core in (fig.7) which has the ability to concentrate the magnetic field thus reducing the leakage flux. With introduction of aluminum shield (fig. 8), it can be observed there is negligible change in the strength of the magnetic field density.

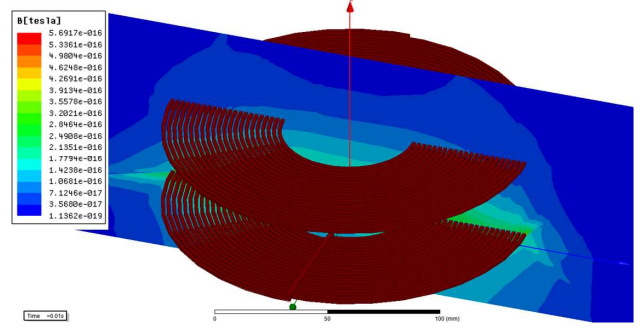


Fig. 6. Magnetic field density plot for Circular coreless transformer

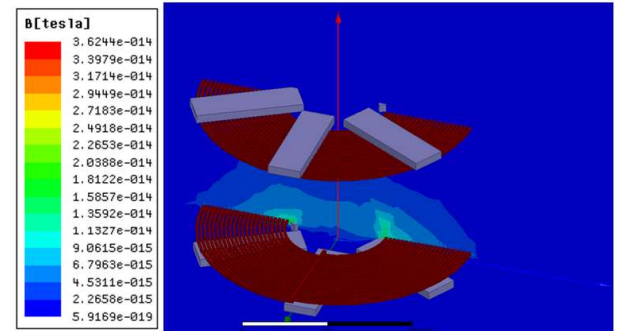


Fig. 7. Magnetic field density plot for circular Ferrite core transformer with no Aluminum shield

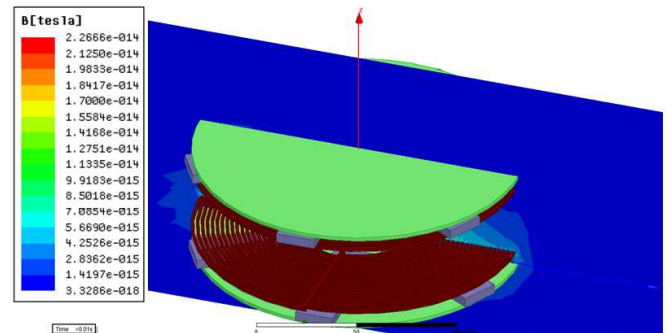


Fig. 8. Magnetic field density plot for Circular Ferrite core transformer with Aluminum shield

The plots reveal that magnetic flux generated by the transmitting coil interacts with that of the receiving coil. The flux density plot in coreless transformer (Fig. 6) indicates extension of the flux above the transmitting coil however in ferrite core transformer (Fig. 7), the flux does not extend much above the receiving coil. This is due to the ability of ferrite to direct the field through it. Further restriction of the flux within the winding region is achieved by placing aluminium shield above the receiving coil and below the transmitting coil (Fig. 8).

IV. RECTANGULAR COIL TRANSFORMER MODELLING AND ANALYSIS

A. FEA Modelling

This section involves 3-D FEA Ansys Maxwell modelling of rectangular coil transformers under three different configurations similar to the circular one in III.

TABLE V
Rectangular coil Transformer dimensions

Winding no. of turns	22
Winding size	Outer-170x170 mm, Inner-60x60 mm
Conductor Thickness	2 mm
Ferrite Bars	4 bars: 65x20x5mm
Aluminum Shield	Area-180x180 mm, thickness-2 mm

Although in general the term rectangular coil transformer is used, the windings of the transformer in table V is a square whose winding area is comparable with the circular coil transformer in table I.

Fig. 9 to fig.11 illustrates Ansys Maxwell models of the rectangular coil with parameters in Table V. A bulk coil model of the winding was used. The number of turns of the coil is defined for the coil geometry during simulation

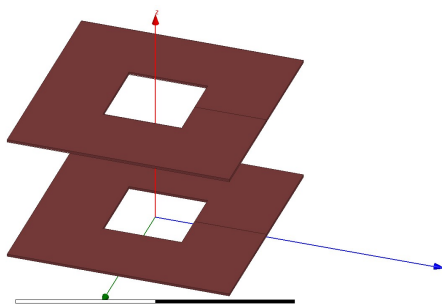


Fig. 9. Rectangular Coreless transformer model

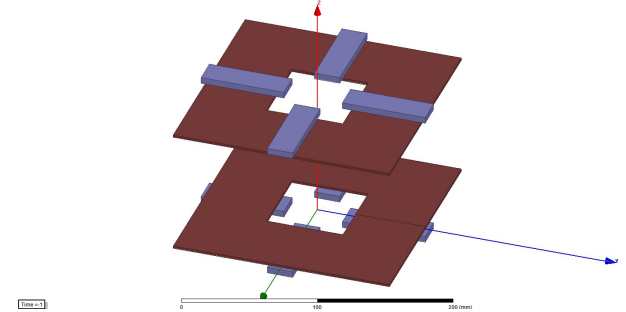


Fig. 10. Rectangular transformer model with Ferrite core only

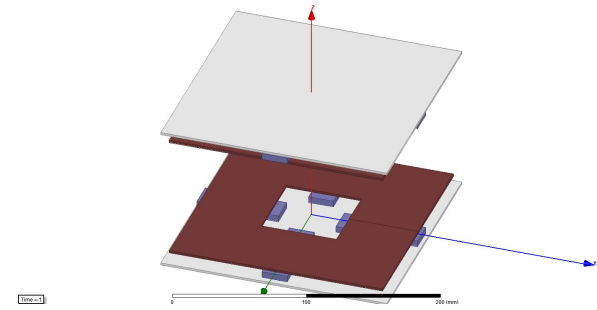


Fig. 11. Rectangular transformer model with Ferrite core and Aluminum shield

B. Simulation results from Ansys Maxwell

TABLE VI
Simulation results from Rectangular Coreless Transformer

<i>d, mm</i>	<i>L₁, μH</i>	<i>L₂, μH</i>	<i>M, μH</i>	<i>k</i>
100	76.42	76.44	6.21	0.08
70	71.66	70.74	9.82	0.12
50	64.79	64.25	14.0	0.22

TABLE VII
Simulation results from Rectangular Core Transformer with no Aluminum shield

<i>d, mm</i>	<i>L₁, μH</i>	<i>L₂, μH</i>	<i>M, μH</i>	<i>k</i>
100	108.17	110.48	12.20	0.11
70	108.24	109.67	21.78	0.20
50	103.72	104.44	34.46	0.33

TABLE VIII
Simulation results from Rectangular Core Transformer with Aluminum shield

<i>d, mm</i>	<i>L₁, μH</i>	<i>L₂, μH</i>	<i>M, μH</i>	<i>k</i>
100	101.50	104.58	10.06	0.10
70	98.54	97.33	18.85	0.19
50	97.85	99.58	31.86	0.32

From these results, it can be noted that rectangular coil parameters vary in the same trend just like those of circular coil discussed in III. Self-inductance L_1 and L_2 have relatively larger values than that of circular transformer. This is because rectangular coil geometry results in longer conducting path as compared to circular coil. Mutual inductance M and coefficient of coupling k is relatively lower than that of a circular coil transformer.

The magnetic field density plot for the three transformers at 50 mm separation between the transmitting and receiving coil is shown fig. 12-14.

The field density plot has the same trend just like in circular coil transformer discussed in section III with the strongest field density observed in fig. 13 (due to the presence of the ferrite core which has the ability to concentrate the magnetic field thus reducing the leakage flux) and the lowest in fig. 12. Similarly the introduction of aluminum shield (Fig. 14), results in negligible change in the strength of the magnetic field density.

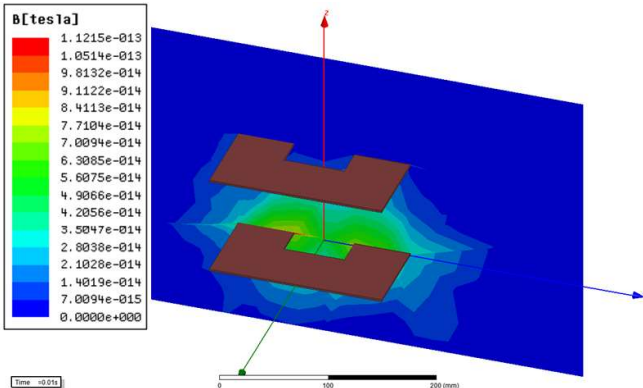


Fig. 12. Magnetic field density plot for Rectangular Coreless coil transformer

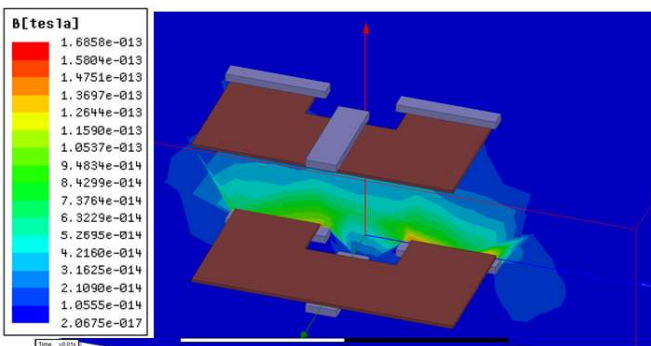


Fig. 13. Magnetic field density plot for Rectangular coil transformer with Ferrite core and no Aluminum shield

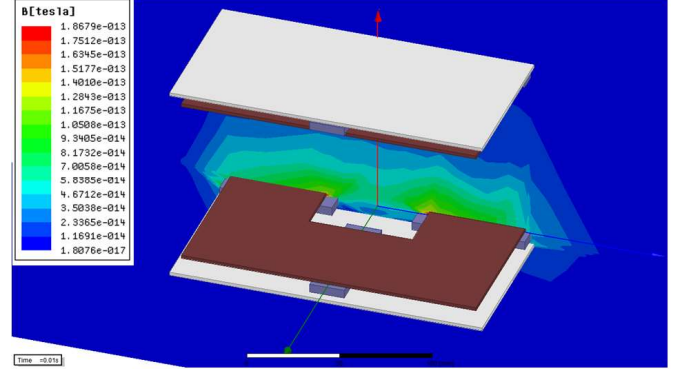


Fig. 14. Magnetic field density plot for Rectangular coil transformer with Ferrite core and Aluminum shield

V. CONCLUSION

In this paper WPT system has been introduced and the parameters of WPT circular and rectangular coil transformer determined and compared using FEA Ansys Maxwell. The magnetic field plots of these transformers under different conditions have also been illustrated. Although in practice L_2 's position relative to L_1 does have some small effect on both inductances, this variation is minimized due to inherently large air gaps used in WPT systems.

From the simulation results it has been shown that coupling between the two coils increases when the separating distance is reduced with circular coil transformer having relatively better coupling as compared to rectangular one with more or less similar dimensions.

ACKNOWLEDGEMENTS

The authors would like to thank University of Cape Town for providing the facilities to accomplish this work.

REFERENCES

- [1] Xiu Zhang; Ho, S.L.; Fu, W.N., "Quantitative Design and Analysis of Relay Resonators in Wireless Power Transfer System," *Magnetics, IEEE Transactions on*, vol.48, no.11, pp.4026,4029, Nov. 2012.
- [2] Chopra, S.; Prasanth, V.; Mansouri, B.E.; Bauer, P., "A contactless power transfer — Supercapacitor based system for EV application," *IECON 2012 - 38th Annual Conference on IEEE Industrial Electronics Society* , vol., no., pp.2860,2865, 25-28 Oct. 2012.
- [3] Neves, A.; Sousa, D.M.; Roque, A.; Terras, J.M., "Analysis of an inductive charging system for a commercial electric vehicle," *Power Electronics and Applications (EPE 2011), Proceedings of the 2011-14th European Conference on* , vol., no., pp.1,10, Aug. 30 2011-Sept. 1 2011.
- [4] Wu, H.H.; Gilchrist, A.; Sealy, K.D.; Bronson, D., "A High Efficiency 5 kW Inductive Charger for EVs Using Dual Side Control," *Industrial Informatics, IEEE Transactions on* , vol.8, no.3, pp.585,595, Aug. 2012
- [5] Hurley, W.G.; Duffy, M.C.; Zhang, J.; Lope, I.; Kunz, B.; Wolfle, W.H., "A Unified Approach to the Calculation of Self- and Mutual-Inductance for Coaxial Coils in Air," *Power Electronics, IEEE Transactions on* , vol.30, no.11, pp.6155,6162, Nov. 2015.

- [6] Madawala, U.K.; Thrimawithana, D.J., "A ring inductive power transfer system," *Industrial Technology (ICIT), 2010 IEEE International Conference on*, vol., no., pp.667,672, 14-17 March 2010.
- [7] Risch, F.; Guenther, S.; Franke, J., "Production concepts for inductive power transfer systems for electric vehicles," *Electric Drives Production Conference (EDPC), 2012 2nd International*, vol., no., pp.1,7, 15-18 Oct. 2012.
- [8] Fariborz Musavi and Wilson Eberle, "Overview of Wireless Power Transfer Technologies for Electric Vehicle Battery Charging," *IET Power Electronics*, vol. 7, iss. 1, pp. 60-66, Jan. 2014.
- [9] Peschiera, B.; Williamson, S.S., "Review and comparison of inductive charging power electronic converter topologies for electric and plug-in hybrid electric vehicles," *Transportation Electrification Conference and Expo (ITEC), 2013 IEEE*, vol., no., pp.1,6, 16-19 June 2013.
- [10] Grant A. Covic and John Talbot Boys, "Modern Trends in Inductive Power Transfer for Transportation Applications," *IEEE Journal of Emerging and Selected Topics in Power Electronics*, vol. 1, no. 1, pp. 28-41, March 2013.
- [11] Zaheer, A.; Covic, G.A.; Kacprzak, D., "A Bipolar Pad in a 10-kHz 300-W Distributed IPT System for AGV Applications," *Industrial Electronics, IEEE Transactions on*, vol.61, no.7, pp.3288, 3301, July 2014.
- [12] Budhia, M.; Covic, G.; Boys, J., "A new IPT magnetic coupler for electric vehicle charging systems," *IECON 2010 - 36th Annual Conference on IEEE Industrial Electronics Society*, vol., no., pp.2487,2492, 7-10 Nov. 2010.
- [13] Mickel Budha, T. Boys and Grant A. Covic, "Development of a Single-Sided Flux Magnetic Coupler for Electric Vehicle IPT Charging Systems," *IEEE Transactions on Industrial Electronics*, vol.60, no. 1, pp. 318-328, Jan. 2013.
- [14] Nagatsuka, Y.; Ehara, N.; Kaneko, Y.; Abe, S.; Yasuda, T., "Compact contactless power transfer system for electric vehicles," *Power Electronics Conference (IPEC), 2010 International*, vol., no., pp.807,813, 21-24 June 2010.
- [15] Budhia, M.; Covic, G.A.; Boys, J.T.; Chang-Yu Huang, "Development and evaluation of single sided flux couplers for contactless electric vehicle charging," *Energy Conversion Congress and Exposition (ECCE), 2011 IEEE*, vol., no., pp.614,621, 17-22 Sept. 2011.
- [16] Mickel Budha, Grant A. Covic and T. Boys, "Design and Optimization of Circular Magnetic Structures for Lumped Inductive Power Transfer System" *IEEE Transactions on Power Electronics*, Vol. 26, No. 11, pp. 3096-3107, Nov. 2011.